Journal Pre-proof

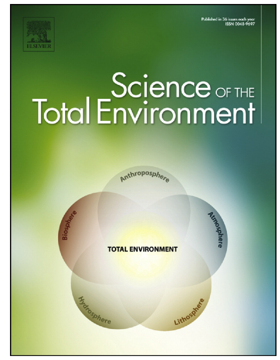

New insights to study the accumulation and erosion processes of fine-grained organic sediments in combined sewer systems from a laboratory scale model

Manuel Regueiro-Picallo, Joaquín Suárez, Esteban Sañudo, Jerónimo Puertas, Jose Anta

PII: S0048-9697(20)30433-2

DOI: https://doi.org/10.1016/j.scitotenv.2020.136923

Reference: STOTEN 136923

To appear in: *Science of the Total Environment*

Received date: 14 November 2019

Revised date: 10 January 2020

Accepted date: 23 January 2020

Please cite this article as: M. Regueiro-Picallo, J. Suárez, E. Sañudo, et al., New insights to study the accumulation and erosion processes of fine-grained organic sediments in combined sewer systems from a laboratory scale model, *Science of the Total Environment* (2020), https://doi.org/10.1016/j.scitotenv.2020.136923

New insights to study the accumulation and erosion processes of fine-grained organic sediments in combined sewer systems from a laboratory scale model

Manuel Regueiro-Picallo[1,*], Joaquín Suárez[1], Esteban Sañudo[1], Jerónimo Puertas[1] and Jose Anta[1]

[1]. Universidade da Coruña, Water and Environmental Engineering Research Team (GEAMA), Civil Engineering School, Elviña, 15071, A Coruña, Spain

*. Corresponding author

e-mail address: manuel.regueiro1@udc.es (Manuel Regueiro-Picallo)

ABSTRACT

The deposition and resuspension of sediments are issues of considerable concern in combined sewer systems management. Sediments can produce the loss of hydraulic capacity and odour generation in sewers, and are also considered the main source of pollution due to their occasional uncontrolled discharges into the environment via Combined Sewer Overflows (CSO). Sewer sediments contain granular and cohesive organic fractions that can have a significant influence on bed resistance. In order to address the relationship between sewer sediment composition and its erodibility, accumulation and erosion experiments were performed in a flume test facility fed with wastewater. The flume was placed in a Wastewater Treatment Plant (WWTP), in which different circular pipe geometries were set. Wastewater flow inlet conditions and bed structures were monitored during the experiments. The photogrammetric technique Structure from Motion (SfM) was applied to record the bed deposit structures, providing accurate measurements of the accumulation rates. The SfM was also used to assess sediment transport and the characteristics of the bed forms after the erosion tests. In addition, velocity distributions and shear stress profiles were measured during the erosion tests to characterize flow resistance and sediment erosion. During both accumulation and erosion tests, sediments were sampled in order to analyse their physicochemical properties, thus highlighting the study of the biodegradability of the organic matter. Different deposition periods showed biological transformations in the bed deposit structure, which were seen to affect its cohesion, and in consequence, its erosion threshold. Tests with significant erosion rates agreed in broad terms with dimensionless sediment transport models derived from previous experimental studies performed with partly cohesive and organic materials in sewer pipes.

KEYWORDS

Bed load transport

Biodegradability

Combined sewers

Erodibility

Photogrammetry

Sewer sediments

1. INTRODUCTION

The combination of sediment deposition, erosion and transport in sewers is an issue of concern in combined sewer systems, and is associated with critical environmental impacts. During dry weather flow conditions, insufficient velocities in sewer conduits produce a sediment layer that reduces their hydraulic capacity. Moreover, the presence of sediment deposits in sewers generates gas and odours, which may have an impact on public health

(Ashley et al., 2004). After long dry weather periods, bed deposits can be eroded by stormwater discharges, resulting in the entrainment of pollutants into the wastewater. The largest discharges may lead to surcharges in the sewer systems and, consequently, to severe impacts on the receiving water bodies (Suárez and Puertas, 2005). Bearing in mind these circumstances, the outlook for the near future is getting worse. Climate change will result in longer dry weather periods with extreme rainfall (Miller and Hutchins, 2017). Without adequate sediment management policies, the impacts of climate change will lead to an increase of depositions in sewers and potentially to the greater presence of pollutants in receiving waters. Therefore, understanding the deposition, erosion and transport processes of in-sewer sediments will help towards reducing pollution episodes with environmental impacts.

The literature which seeks to describe sediment transport in sewers is extensive. Most studies were performed in field campaigns, and in general were based on the classification of the deposited sediments and the origin of pollutant loads in combined sewers (Crabtree, 1989; Verbanck, 1990; Chebbo and Bachoc, 1992). Such studies showed that the presence of organic content in sewer sediments exhibited properties that were different from granular materials. In addition, the erosion of these organic in-sewer sediments during dry weather conditions was shown to be the main source of pollution in Combined Sewer Overflow episodes (CSOs) (Ashley and Crabtree, 1992; Ahyerre et al., 2001; Gromaire et al., 2001). Thus, high pollution loads are originated by the re-suspension of the highly biodegradable organic matter content of gross sediments beds (Sakrabani et al. 2009), which may result in depletion of dissolved oxygen in receiving waters. Furthermore, sewer sediments deposits are considered as a stock of other pollutants such as heavy metals (Rocher et al., 2004; Houhou et al., 2009), different forms of organic pollution such as PAHs (Rocher et al., 2004), PCBs, flame retardants or pesticides (Schertzinger et al., 2019) and even PPCPs and illicit drugs (Del Río et al., 2013; Munro et al., 2019) that can be found in receiving waters.

Along with field campaigns, laboratory studies have also been reported. Experiments were performed under controlled conditions to address the issue of sediment transport models in sewers, which were historically based on formulas proposed for alluvial sediments (Bertrand-Krajewski, 2006). The earliest attempts were carried out in pipe channels with non-cohesive materials (Perrusquía 1992; May, 1993; Nalluri et al., 1994; Ackers, 1996). However, significant differences were shown between non-cohesive model approaches derived from experiments with uniform sands, and measurements performed in sewers (Arthur et al., 1996; De Sutter et al, 2003). As an approximation to sewer sediment characteristics, cohesive mixtures were also used to study erosion processes in laboratory scale models (Torfs, 1994; De Sutter, 2000; Banasiak and Verhoeven, 2008; Campisano et al., 2008). Even surrogate materials, such as crushed olive stones, were used as a means of trying to reproduce the cohesion of sewer sediment (Tait et al., 1998; Skipworth et al., 1999). Nevertheless, most laboratory experiments ignored the influence of organic content during the deposition phase and its interaction with the wastewater flow.

Some research introduced the biodegradation of sewer sediments, this produced by organic processes, as a key parameter in explaining sediment erosion in combined sewers (Vollertsen and Hvitved-Jacobsen, 2000). For that purpose, reduced laboratory-scale erosion meters were developed, in which the relationship between the eroded mass and the shear stress conditions were analysed in terms of the consolidation time of the sample and the oxygen supply conditions (Sakrabani et al., 2005; Schellart et al., 2005; Seco et al., 2014; Meng et al., 2019). The transformations derived from the biological activity in sewer sediment samples produced differences in bed resistance. A recent example is the work performed by Meng et al. (2019) which analyse the effect of extracellular polymeric substances (EPS) and microbial community on the anti-scouribility properties of sewer sediments. These authors found some positive correlations between the EPS, proteins, carbohydrates and microbial community content for the improvement of sediment strength to flow erosion. A smaller number of studies looked at the relationship between sediment cohesiveness, consolidation and bed resistance in gravity pipe flows with sewer sediments (c.f. Tait et al. 2003 and Banasiak et al. 2005), but the influence of the wastewater flow in the sediment deposition processes here was almost wholly ignored.

Experimental facilities that operated with wastewater aims to avoid some of the previous works limitations. Various examples of test facilities were identified, in which gravity pipes were supplied with wastewater from a local sewage or a Wastewater Treatment Plant (WWTP) (Rushforth et al., 2003; Lange and Wichern, 2013). Other flume configurations included annular flumes with rectangular sections. These were also used to study the critical shear stress in cohesive sediments and the variability produced by the wastewater supply conditions (Maa et al., 2008; Khastar-Boroujeni et al., 2017). Such configurations produced disturbances in the water depth due to the intrusive flowrate generation system. Also, the shear stress produced in annular flumes differed from that in circular pipes.

The relationship between sediment cohesion and its effect in bed strength is still unclear for sewer sediments (Banasiak et al. 2005, Meng et al. 2019). Also, the presence of organic matter in sewer sediments produces continuous transformations in bed deposits that modifies their resistance. Therefore, the current study aims to address the relationship between sediment biodegradability and its cohesion, considering accumulation and erosion conditions. For this purpose, new approaches were developed to obtain accurate measurements of bed structures and the physicochemical properties of sediments.

A compilation of various deposition and sediment transport experiments will be described in this study. To this end, a flume test facility at the WWTP of A Coruña (Spain) was used. The first studies performed in this facility were presented in Regueiro-Picallo et al. (2017). These focused on monitoring sediment deposition in sewer pipes and how this accumulation affected velocity and shear stress distributions. Subsequently, the experimental campaign reported in Regueiro-Picallo et al. (2018) introduced sediment transport tests after the deposition phase.

These tests focused on sediment 'aging' and biodegradability in small pipe diameters, and their influence on bed resistance when shear stress conditions were increased. The current work introduces additional deposition and transport tests with different time scales, in order to study in depth the influence of variations in sediment properties on the bed-load transport. Furthermore, bed forms were identified in the sediment transport tests, and their dimensions were related to bed resistance. Finally, results from transport tests were compared with bed-load transport models to predict the mobilised mass of sewer sediments.

2. MATERIAL AND METHODS

The test campaign was performed in a flume test facility fed with wastewater. This facility offers different supplying systems to control the wastewater inlet conditions. Another advantage is the possibility of setting different pipes in order to obtain representative results from the typical diameters used in secondary sewer systems. Innovative methodologies are also employed to obtain the volume of bed deposits and to analyse the physicochemical properties of the sediment samples. Finally, the experimental procedure for studying the accumulation, erosion and transport processes is described.

2.1. Description of the flume test facility

2.1.1. Flume overview

The flume test facility was built with the aim of studying sediment transport in sewer pipes. The flume presents a metallic bench with a length of 10 m and a width of 0.8 m. The studied sewer pipes were placed over the bench and have a length ranged from 7.5 to 8.0 m. The pipe slopes were set below 0.5% in order to favour accumulation conditions.

The principal advantage of this flume is that real wastewater can be supplied from the pretreatment system of the WWTP to the inlet tank of the facility. Wastewater flow is then split through two v-notch weirs and falls into a discharge chamber before going through each pipe. After flowing along the pipes, wastewater is discharged in a downstream chamber where an automatic tailgate is placed to set downstream boundary conditions.

The facility was equipped for monitoring wastewater loads and hydraulic variables with several probes, and for analyzing sediment composition (Figure 1). Wastewater loads were monitored in the inlet and downstream tanks of the flume with online probes that measured turbidity (SOLITAX, Hach, USA) and light absorbance (UVAS, Hach, USA). These continuous recordings were compared with the wastewater Total Suspended Solids (TSS) and Chemical Oxygen Demand (COD) concentrations, respectively. These parameters were analyzed from samples taken with an autosampler (SIGMA900, Hach, USA), the nozzle of which was placed near the online probes.

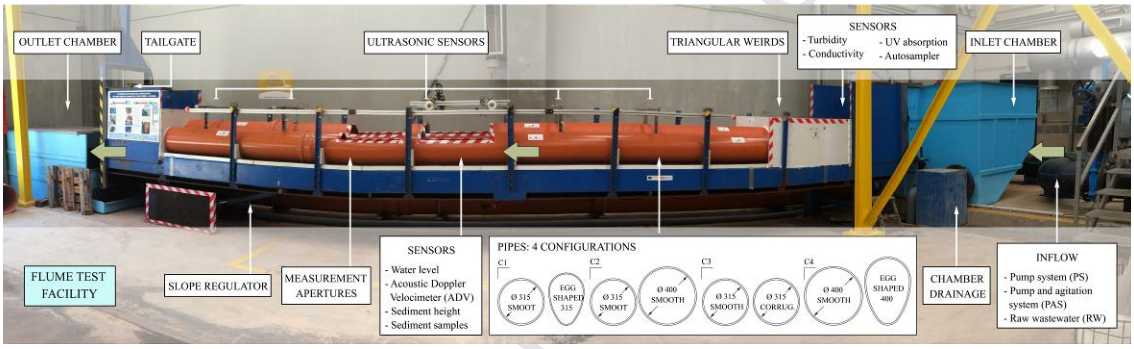

Figure 1. Scheme of the flume test facility.

The inlet discharge was calibrated comparing the water level in the inlet tank with an ultrasonic flowmeter (TDS-100H, PCE Instruments, Germany) placed in the pumping supplying system. Furthermore, ultrasonic water depth sensors (UB500-18GM75-I-V15, Pepperl+Fuchs, Germany) with a resolution of 0.13 mm were used for measuring the water depths along the pipes, and also for recording the level in the inlet tank. Small apertures were opened in the pipes for installing the water depth ultrasonic sensors at 1.5, 2.5, 5.5 and 6.5 m from the pipe inlet. As well as the continuous recordings, periodic measurements of velocity profiles and sediment characteristics were recorded in the pipes. Centerline velocity profiles were measured with an Acoustic Doppler Velocimeter (Vectrino, Nortek, Norway). In addition, photogrammetric techniques and sampling analyses were developed to obtain sediment volume and composition, respectively. For this purpose, two main windows were also opened up at 3.2 to 4.8 m from the pipe inlet.

2.1.2. Wastewater inlet conditions

Different supply conditions were available in the facility in order to feed wastewater to the inlet tank: pump system (PS), pump system and agitation (PS+A), and raw wastewater (RW). On the one hand, a pressured pipe circuit was used to pump the wastewater from the primary screening deposit of the WWTP. Under this configuration, constant flowrate conditions could be assured during the tests and particle diameters were limited to the 3 mm grid aperture of the sieves. Therefore, some particle sizes and gross solids were missed. Additionally, particle settling was identified at the inlet tank due to low agitation conditions. Therefore, some experiments were performed with an agitation pump installed close to the bottom of the inlet tank in order to resuspend sediments. On the other hand, raw wastewater could also be provided using a gravity system from the inlet chamber of the pretreatment facility. Complete grain size distributions were supplied and thus cloths and fibres were also observed with this set up. The resuspension system could not be turned on under raw wastewater supply conditions, this in order to avoid clogging of the agitation pump.

2.1.3. Sewer pipes set-up

Sediment transport experiments were performed using 315 mm corrugated and 315 and 400 mm smooth PVC pipes placed on the flume. The inner diameters (ID) of these pipes were 275, 300 and 380 mm, respectively. These diameters are the most common geometries used in the upper side of urban catchments, what Rammal et al. (2017) have defined as upstream secondary sewers, which significatively contribute to the sediment load in case of particle resuspension.

The width of the flume test facility makes it possible to set two sewer pipes at the same time. Therefore, the experimental campaign was divided into four flume configurations. The corrugated and the smooth 315 mm pipes were tested simultaneously, as were the 315 and the 400 mm smooth pipes. Also, 315 and 400 mm smooth pipes were compared with equivalent egg-shaped pipes, respectively. No significant bed deposit accumulation was observed in tests performed with the egg-shaped pipes, in line with results previously reported in Regueiro-Picallo et al. (2017). Therefore, the present study focused solely on results derived from the circular pipes.

2.2. Determination of bed structure and sediment properties

2.2.1. Measurement of sediment deposits

Different methodologies were applied to record the volume of sediments deposited in the pipe contour. Before doing so, pipes were drained carefully, and in this way the sediment deposits remained undisturbed. First, the methodologies applied in the pipes consisted of measuring the bed sediments with the same ultrasonic sensors used for water depths, and sediment profiles were obtained from processed images from a laser pointing at the pipe contour. This second method improved the punctual recordings from the ultrasonic sensors showing the boundaries between the sediments and the pipe contour. However, it also revealed a lack of information about the bed deposits along the pipe, in that three-dimensional structures were observed in most of the tests. More details about these methods are available in Regueiro-Picallo et al. (2017). In order to obtain more accurate information about the sediment deposits, an innovative solution was applied using the Structure from Motion (SfM) technique. SfM is based on photogrammetric methods and allows a 3D reconstruction model to be obtained from a set of images (see details in the Supplementary Information to this article). This methodology was briefly introduced in Regueiro-Picallo et al. (2018) for the same purpose of measuring sediment accumulation and bed formations; prior to this, there seem to be no references in the literature to the application of such a technique in the sanitary system research field. Another recent example of the application of SfM in the urban drainage field can be found in studies by Naves et al. (2019a, 2019b), which used this technique to obtain the topography of a laboratory street model to simulate surface run-off and to calculate velocity map distributions.

2.2.2. Sediment physicochemical analysis

Sediment samples were collected manually from the main apertures of the pipes. Afterwards, these samples were transferred to the laboratory and frozen so that their properties remained undisturbed prior to analysis. The physicochemical properties of sediment samples were analysed following international standards. Solid fractions (Total Solids- TS and Volatile Solids- VS) and moisture content, together with sediment density and grain size distribution, were the physical parameters analysed. Wet and particle densities were obtained following the APHA (1998) and UNE-EN 1097-6:2014 (AENOR, 2014) standards. However, the differences between the two procedures were below 1%. Therefore, only values from the APHA (1998) procedure will be shown in the results. Also, a laser diffraction device (Beckman Coulter, USA) was used to analyse the grain size distribution (ISO 13320:2009). Laser diffraction analysis presents a higher size class resolution with a maximum grain size of 2 mm particles. Despite this limit, all the sediment samples showed lower particle sizes.

Chemical Oxygen Demand (COD) and Oxygen Uptake Rate (OUR) were also analysed. For this, sediment samples needed to be prepared through a dilution of the sample with distilled water. Three COD types were defined following McGregor et al. (1993) and Regueiro-Picallo et al. (2018), according to the agitation applied to the sample dilutions during the preparation processes. An absolute value of the sediment COD was obtained after blending the solid-water dilution (COD type I), whereas an estimation of the erodible COD from the bed deposits resulted from mixing and stirring (COD type II and III). Furthermore, OUR is a relative value of the oxygen consumption obtained from respirometry analysis. This variable derives from the BOD regression after 48 hours, similar to that reported in Sadaka et al. (2006), and shows how fast the degradation of the sediment sample occurs.

2.3. Experimental procedure

2.3.1. Accumulation tests

The accumulation tests were performed by applying disadvantageous hydraulic conditions in the pipes in order to favour sediment deposition. These conditions were set during different dry weather flow periods between 3 and 21 days (Figure 2). The aim of testing different deposition periods was to study the evolution of the sediment characteristics, thus continuing studies by Regueiro-Picallo et al. (2018).

The three types of wastewater supply conditions mentioned above were performed in this set of experiments. Flowrate, pipe slope, and downstream boundary conditions were fixed at the beginning of each test, and were kept constant during the accumulation phase. Wastewater discharges were tested from 1.8 to 4.7 L/s, pipe slopes were set below 0.7%, and the fixed downstream boundary conditions resulted in water depths between 75 mm and 110 mm in the central main aperture.

Regular visits to the facility were programmed in order to collect continuous monitoring data and perform measurements of sediment composition. For the latter, wastewater discharge was by-passed and the pipes were slowly drained so that the volume of sediments could be measured and samples taken. In some of the experiments, the remaining sediments at the end of the deposition phase were taken as the initial conditions to perform erosion tests, and for the remaining accumulation tests, the pipes were cleaned and returned to their initial state.

2.3.2. Erosion tests

The erosion tests were performed by increasing the flow conditions from the accumulation phase. The erosion phase started once the flowrate was increased. These flow conditions were kept constant for 30 minutes for all the experiments, following similar experimental procedures to those in previous studies (Rushforth et al. 2003, for example). Some of the erosion experiments were performed sequentially by applying velocity increases with the aim of setting different shear stress conditions in the near-bed layer (Figure 2). Although the discharge was fixed at 12 L/s on average for all the erosion tests, the near-bed shear stress conditions were increased by reducing the downstream boundary condition. During the sediment erosion, centreline velocity and shear stress profiles were recorded with the ADV. Once the erosion step had finished, pipes were drained again, and the volume of sediments were measured and samples were collected. The uneroded sediments were the initial conditions in the next erosion step.

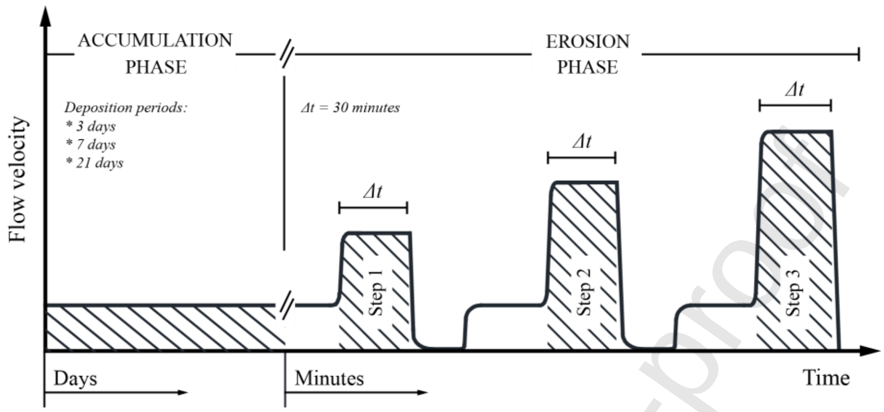

Figure 2. Experimental procedure for the accumulation and erosion phases.

2.4. In-sewer sediment transport and erosion models

A wide variety of formulas can be applied to predict in-sewer sediment mobility. These formulas are commonly related to the flow bottom shear stress availability to scour sediments beds. However, two sediment transport modes can be distinguished between granular and fine fractions. The transport of granular materials, which can be divided into bed and suspended loads, depends on flow conditions and the physical properties of the deposited particles. Conversely, the erosion of fine cohesive sediments is expressed through the relationship between the erosion rate and the critical shear stress, which indicates their incipient motion (Skipworth et al., 1999). In the present study, the sewer sediment presented partly organic and cohesive properties. Under these conditions, few models provide reliable sediment transport predictions. The erosion mode that will be used hereon is the bed load sediment transport, which is based on the bed resistance. Following the procedure described by Banasiak and Verhoeven (2008), this approach presents the best fit for the near bed layer mobilization of partly cohesive particles and sands in circular pipes.

The sediment bed resistance was evaluated with the bed shear stress, which depended on the hydraulic characteristics and the initial sediment conditions. The bed shear stress was estimated from the centreline velocity profiles recorded with the ADV during the erosion tests, similar to the procedure in Tait et al. (2003) and Oms et al. (2008). The velocity profiles were obtained from 8 to 12 points measured from the wastewater surface to the near-bottom with a point distance between 5 and 10 mm. The three orthogonal velocity vectors were measured with a sampling frequency of 25 Hz for 60 seconds at each point. In addition, the phase-space thresholding method proposed by Goring and Nikora (2002) was applied to de-spike the velocity measurements. As a result, the bed shear stress can be expressed by the maximum of the linear Reynolds shear stresses distribution near the bed surface:

$$\tau_b = -\rho\overline{u'w'} \tag{1}$$

where ρ is the fluid density (kg/m^3) and u' and w' are the velocity fluctuations on the *x* and *z* axes, respectively. The velocity fluctuations are defined as $u'(t) = u(t) - \overline{u}$ and $w'(t) = w(t) - \overline{w}$, where $\overline{u}$ and $\overline{w}$ are the average velocities in the *x* and *z* axes for each measurement. The bed shear stress for mobile beds is commonly expressed as the composition of the grain and form resistances $\tau_b = \tau_b' + \tau_b''$, corresponding to the skin friction and the bed form shear stress, respectively. The skin friction shear stress is estimated from the expression ${\tau'}_b = \rho {u_*'}^2$, where u_*' is the grain shear velocity that can be evaluated for rough-bed experiments with the Manning-Strickler equation (Banasiak and Verhoeven, 2008):

$$\frac{U_0}{u_*'} = 8.1\left(\frac{R_b}{k_s'}\right)^{1/6} \tag{2}$$

where U_0 (m/s) is the initial mean velocity of the experiment, k_s' is the equivalent bed roughness height regarding the grain size and is assumed to be equal to the mean grain size d_{50} of the bed deposits (Banasiak and Verhoeven, 2008), and R_b is the hydraulic radius influenced by the bed deposit that can be obtained from the sidewall elimination approach:

$$R_b = R\left(\frac{n_b}{n_{eq}}\right)^{3/2} \tag{3}$$

where R is the total hydraulic radius and n_{eq} and n_b (s/m$^{1/3}$) are the roughness coefficients. The composite roughness n_{eq} is determined based on the Einstein (1942) approach:

$$n_{eq} = \left(\frac{P_w \cdot n_w^{3/2} + P_b \cdot n_b^{3/2}}{P}\right)^{2/3} \quad (4)$$

where P (m) is the wetted perimeter and the subscripts w and b denote the pipe wall and the sediment bed, respectively. Therefore, the composite roughness n_{eq} is equal to the PVC wall roughness n_w when no sediment is deposited in the pipe. The value of the n_w was fixed at 0.010 s/m$^{1/3}$, which is a common value for clean PVC pipes, and the bed roughness n_b was obtained using the Strickler's equation as a function of the mean grain size d_{50} (m) of the sediments:

$$n_b = \frac{{d_{50}}^{1/6}}{21.1} \quad (5)$$

3. RESULTS

This section will show the wastewater flow loads at the inlet tank of the facility, taking into consideration the operational strategies of the WWTP. Then, the results of the deposition and sediment transport tests will be presented separately. Accumulation results focus on the deposition rate of sediments in the bottom of the pipes, the description of the type of in-sewer sediments, and the time-evolution of their physicochemical properties. By contrast, transport tests show the influence of flat or bed form conditions in the shear stress distributions in pipes. Bed form dimensions are also measured and their influence in the flow resistance is noted. Finally, dimensionless bed-load transport rates are compared with predictions derived from former transport capacity formulas.

3.1. Inlet wastewater characterization

The facility allowed for fixing roughly constant flowrates, but the wastewater concentrations were influenced by variations in the wastewater load. TSS and COD daily patterns were observed using wastewater probes. Conversely, rain events do not affect the facility's wastewater supply, due to the flow homogenization capacity of the WWTP (Regueiro-Picallo et al., 2017). TSS and COD concentrations were obtained from the wastewater sampling campaign. Daily TSS concentrations ranged from 50 to 550 mg/L and COD values from 50 to 1300 mg/L. Turbidity and light absorbance recordings from the probes were compared with the TSS and COD concentrations in each test, respectively. A significant variability between Turbidity-TSS (Figure 3, a and b) and Absorbance-COD (Figure 3, c and d) relationships was observed due to the heterogeneous composition of the wastewater.

In terms of the wastewater supply conditions, the average TSS and COD concentrations were 236 and 519 mg/L, respectively, in the tests performed with the pump system. The concentrations slightly increased to 247 and 548 mg/L, respectively, when the agitation pump was enabled in the pump system and agitation tests. Finally, the raw wastewater supplying system provided the highest TSS and COD concentrations of 355 and 818 mg/L, respectively. These differences in the inlet wastewater parameters, especially in the suspended solid concentrations, influenced the volume of deposited sediments, as will be shown below.

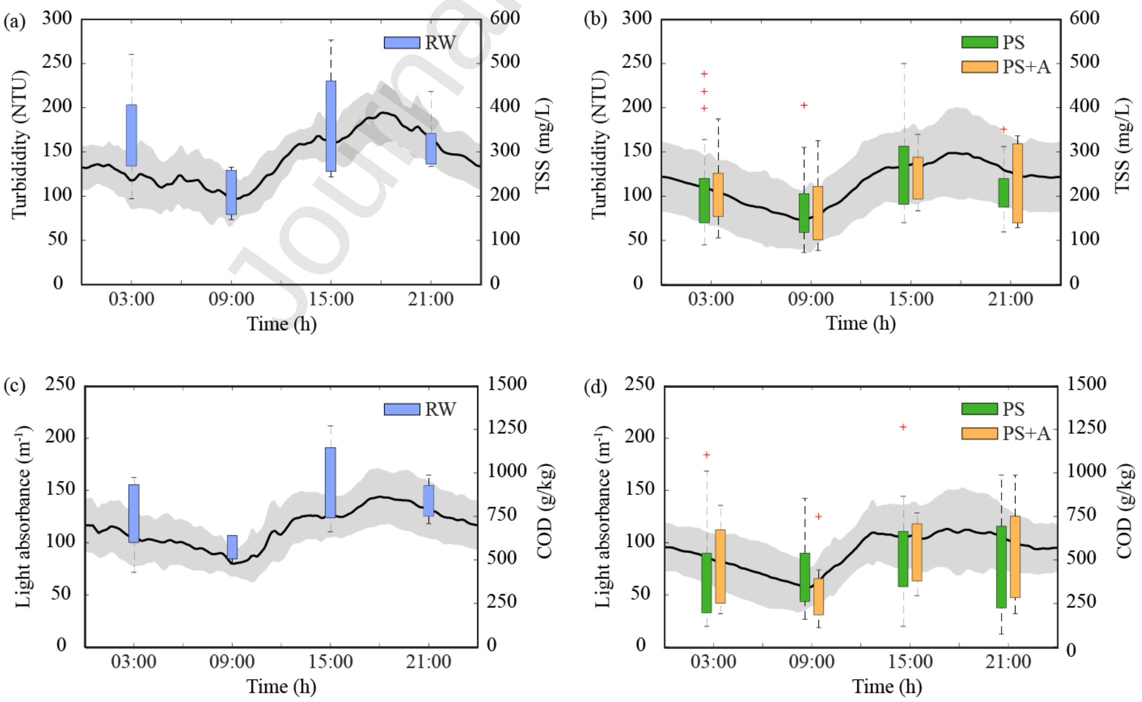

Figure 3. Comparison of performance in the facility's inlet tank between the average (black line) ± standard deviation (grey shade range) daily signals of turbidity (a and b) and light absorbance (c and d) probes, and the analysed wastewater parameters TSS and COD, respectively. Wastewater parameters are represented by boxplots, where the box represents the 25th and 75th percentiles of the values, the dash-line covers values that are less than

1.5 times the interquartile range from the top or bottom of the box, and red '+' signs are outliers. Boxplots are separated according to RW (blue), PS (green) and PS+A (orange) supply conditions.

3.2. Sediment accumulation tests

3.2.1. Evolution of sediment bed deposits

A series of 28 accumulation tests were performed in the flume test facility, involving the three inner diameters (ID) of the circular pipes. Different deposition times were studied; short periods between 3 and 7 days, and long accumulation terms for more than 10 days of dry weather flow conditions. As mentioned earlier, constant flowrates were set during the tests, according to the three wastewater supply conditions. In addition, disadvantageous slopes and downstream boundary conditions produced low mean velocities that favoured the deposition of sediments in the bottom of the pipes. The threshold mean velocity that caused the sediment accumulation was roughly estimated at 0.3 m/s, in light of results reported in Regueiro-Picallo et al. (2017). In the present study, all the accumulation tests were performed with a lower flow velocity. The complete accumulation test conditions are provided in Table S1 in the Supplementary Information to this article.

The deposition rate represents the linear increase of the bed deposit height during the first days of accumulation. This approach was limited to seven days in the case of large periods, which showed non-linear sediment growths once the first week of the deposition test had passed, as illustrated below. The sediment accumulation was obtained from the volume of bed deposits recorded during the deposition processes at the central control section of each pipe. The most accurate results were obtained by applying the SfM method, this due to the complete reconstruction of the bed deposits (Regueiro-Picallo et al., 2018). Such a procedure allowed for the calculation of the total volume of the sediments deposited in the control section and also the forms on the bed surface. Therefore, the average sediment height was calculated according to the circular segment formula.

Figure 4 shows the time-evolution of the bed deposit heights in the 315 (smooth and corrugated) and 400 mm pipes, regarding the wastewater supply conditions. The resulting deposition rates ranged from 0.8 to 6.2 mm/day during the first week. The highest growth rates corresponded to the experiments performed with the raw wastewater supply conditions, which presented the lowest initial mean velocities and the highest TSS inlet concentrations. Under these conditions, the deposition rate increased to 4.9 mm/day on average. In the remaining tests performed with the pump system, different decay trends in the sediment height values were observed after the linear increase during the first week. The 315 mm pipe results decreased after the tenth day of deposition, which might be assumed as a result of the compacting of the bed deposit layer, similar to that reported by Banasiak et al. (2005). Conversely, the 400 mm pipe measurements stabilized at a constant sediment height of 20 mm from the fifteenth day.

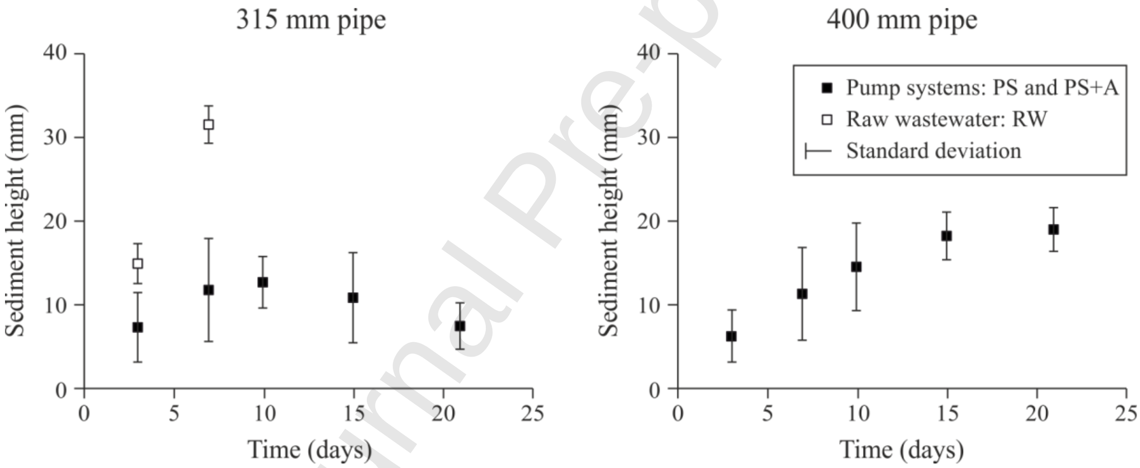

Figure 4. Sediment deposition during the accumulation phase in the 315 and 400 mm pipes.

3.2.2. Characterization of the sediment physicochemical properties

A total of 88 samples were collected in order to analyse the physicochemical properties of the in-sewer sediments during the deposition campaign. Sediment sampling was performed, as a minimum, at the end of each accumulation test. However, control samples were also taken during the deposition phase in some experiments. The types of in-sewer sediments identified were bed deposits (44 samples), which were deposited at the bottom of the pipes, and wall biofilms (44 samples). They were classified as type A/C and type D sediments respectively, according to the sewer sediment rank proposed by Crabtree (1989). Most of the parameters from the physicochemical analysis of the sediment samples showed an average ± standard deviation (SD) similar to past studies, with some exceptions (Table 1). The COD values from bed deposit samples were slightly lower than those obtained by Crabtree (1989). The same applied to the volatile fraction, COD and OUR parameters in wall biofilms, although the presence of organic particles was higher than in bed deposit samples.

Table 1. Physicochemical properties of bed deposits (Type A/C) and wall biofilms (Type D) in the deposition tests, and comparison with past studies.

Parameter	**Bed deposits**			**Wall biofilms**	
	Average ± SD	Type A[1)]	Type C[1)]	Average ± SD	Type D[1)]
Wet density (kg/m^3)	1409 ± 143	1720	1170	1145 ± 79	1210
TS (g/kg)	480 ± 122	734	270	249 ± 59	258
VS/TS (%)	17.5 ± 14.6	7.0 ± 5.4	50.0 ± 23.5	21.5 ± 7.4	61.0 ± 32.9
d_{50} (mm)	0.149 ± 0.044	0.063-2	0.063-2	0.043 ± 0.010	0.063-2
COD type I (g/kg)*	11.1 ± 18.1	23 ± 14.5	76 ± 17.5	34.1 ± 21.1	193 ± 160.2
COD type II (g/kg)*	7.7 ± 15.5	-	-	21.0 ± 12.8	-
COD type III (g/kg)*	8.3 ± 14.9	-	-	23.4 ± 14.7	-
OUR (g/kg/d)*	15.2 ± 15.2	4.2 ± 3.8	20 ± 10.2	37.9 ± 12.7	103 ± 97.9

1) Adapted from Crabtree (1989). *(g/kg) and (g/kg/d) dry sediments

Regarding the standard deviations from the average values, the parameters related to the organic content showed a high degree of variability, most notably in bed deposit samples. The reason for such fluctuations derives from the time-evolution transformations of the sediments. Figure 5a shows that the bed deposit samples with the largest organic content were obtained during the first week. Later, the organic content decreased as the accumulation period increased. The volatile content presented an average percentage of 24% during the first week, reaching values close to the 70% of volatile solids during the first three days. Then, the percentage decreased to 14% and 10% during the second and third weeks, respectively. Likewise, COD and OUR parameters followed the same decreasing trends. During the first week the COD type I and the OUR were 18.6 g/Kg and 23.0 g/kg/day, respectively. The results then decreased to 7.2 g/kg and 11.1 g/kg/day during the second week. Finally, the analysis of chemical parameters showed a decrease to 4.3 g/kg and 6.6 g/kg/day in the third week. The same trend was reflected in the COD type II and III analysis, which represented 83% and 89% on average of the COD Type I values, respectively (R^2 = 0.97 in both cases).

Opposite trends were obtained for the total solids and wet densities of the bed deposits (Figure 5b): the larger the deposited period, the greater the solid content and density. These parameters increased from 43.2 g/kg and 1356 kg/m^3 in the first deposition week, to 50.2 g/kg and 1432 kg/m^3 in the second week, and 53.8 g/kg and 1469 kg/m^3 in the third week, respectively. Based on these results, the sediment consolidation tended to minimize the organic fraction of bed deposits. Regarding the particle distributions, the mean grain size values decreased slightly on average during the accumulation phase, from 0.164 mm in the first week to a constant value of 0.140 mm in the following deposition periods. As a result of the complete analysis of bed deposit samples, the volatile content showed clear relationships with the oxygen consumption indicators (COD and OUR) and also with the wet density and particle size distribution parameters (see Figure S2 in the Supplementary Information to this article).

Smaller time variations of the wall biofilm physicochemical properties were obtained compared to that for bed deposits (Figure 5, c and d). The volatile content in the biofilm samples during the deposition phase decreased from 24.5 ± 8.2% during the first week, similar to the bed deposit samples, to a constant value of 18.9% (± 8.2% and 4.4%) in the second and third weeks. Similar decays were also obtained for the COD and OUR parameters, the average values of which were greater than those for the bed deposits. Thus, the COD type I began with a value of 50 ± 33.9 g/kg, then decreased to 26.5 ± 9.7 g/kg during the middle-week, and reduced further to 19.3 ± 2.1 g/kg at the end of the largest accumulation tests. Likewise, the OUR analysis showed a value of 43.9 ± 11.5 g/kg/day in the first week and decreased to 36.6 ± 13.2 g/kg/day and 27.1 ± 8.3 g/kg/day during the second and third weeks, respectively.

Regarding the physical parameters, results were lower than those obtained for bed deposits and were constant, without being influenced by the deposition time.

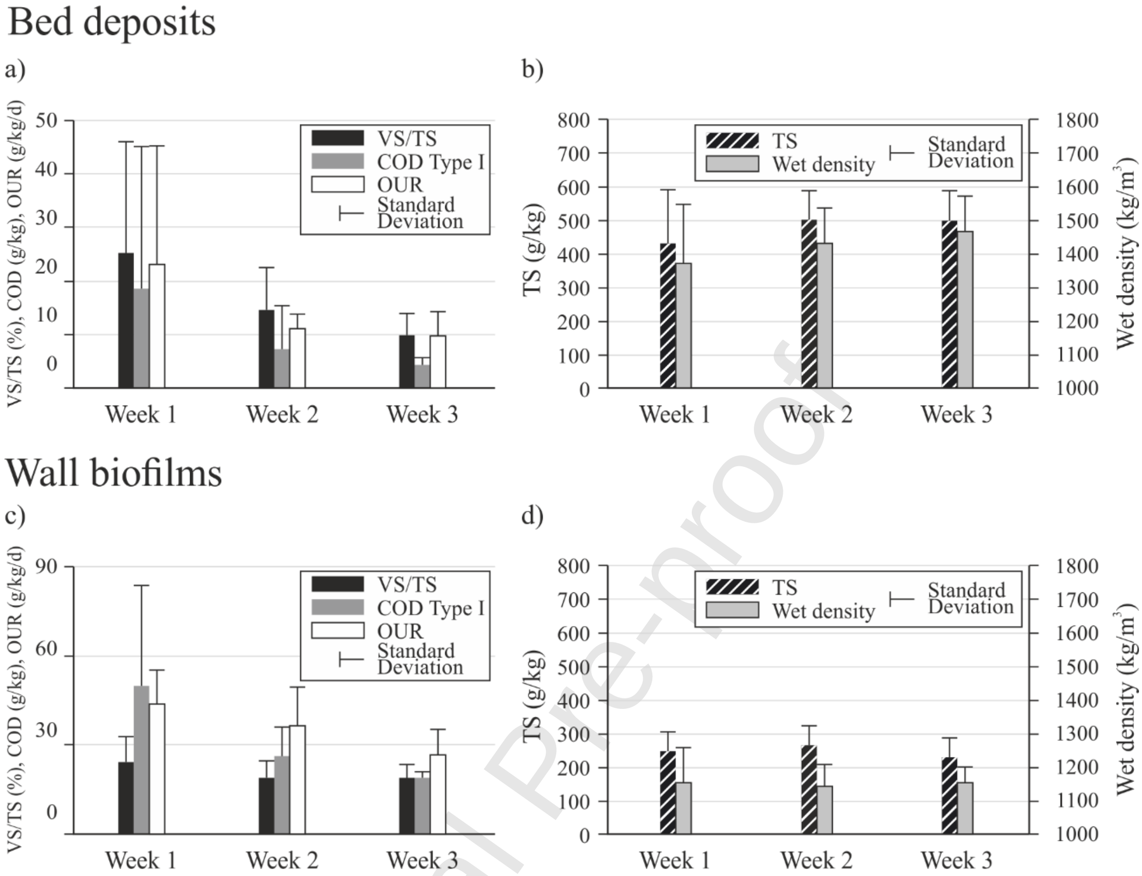

Figure 5. Time-induced variations in the mean and standard deviation values of the physicochemical properties (volatile content, COD type I, OUR, total solids and wet density) of bed deposits (a and b) and wall biofilms (c and d).

3.3. Sediment erosion tests

3.3.1. Bed forms

Bed forms are produced in erodible sediment deposits under certain flow and sediment transport conditions. The velocity conditions in the sediment erosion tests ranged from 0.30 to 0.57 m/s, which led to different Froude numbers $F = U_0/(gA/B)^{0.5}$, where A (m^2) is the wetted area and B (m) is the width of the water surface. Bed forms were identified with Froude numbers between 0.30 and 0.40 for the tests performed in the 315 mm smooth and corrugated pipes, and between 0.35 and 0.50 in the 400 mm smooth pipe. Finally, experiment conditions that produced Froude numbers greater than 0.55 resulted in the complete washing out of the deposited particles. Further details of the erosion test conditions can be found in Table S2 in the Supplementary Information.

These bed structures were distributed repeatedly on the longitudinal axis but also had transverse variations. The SfM methodology improved the accuracy of determining the average bed form amplitude H_{bed} and wavelength L_{bed} from the spatial bed-form distribution after each erosion run. Figure 6a shows the spatial-averaged profiles of the ripples and dunes from different erosion test conditions. The bed forms for the complete set of experiments present heights of between 1.3 and 4.4 mm and lengths of between 25.8 and 45.6 mm.

Following the criteria proposed by García (2008), the bed forms in the present study can be classified as ripples, because all the tests satisfied the conditions $F < 1$ and $Re^* \leq 11.6$, where $Re^* = u_* d_{50}/\nu$ is the shear velocity Reynolds number, u_* is the total friction velocity (m/s), and ν is the water dynamic viscosity (m^2/s). The total friction velocity can be estimated from $u_* = \sqrt{gRS_f}$, where S_f is the friction slope determined by the Manning equation $U_0 = R^{2/3}\sqrt{Sf}/n_{eq}$. Under these conditions, ripple dimensions depend mainly on the bed deposit characteristics. Figure 6b shows the relationship between the ripple steepness and the dimensionless particle diameter $D^* = d_{50}(g(\rho_s/\rho - 1)/\nu^2)^{1/3}$. The ripple steepness, which is commonly related to the bed resistance (van Rijn, 1984), decreased with the larger grain sizes, as suggested in previous studies (e.g. Raudkivi, 1997). More details about the dimensions of the bed forms can be found in Figure S3 in the Supplementary Information to this article.

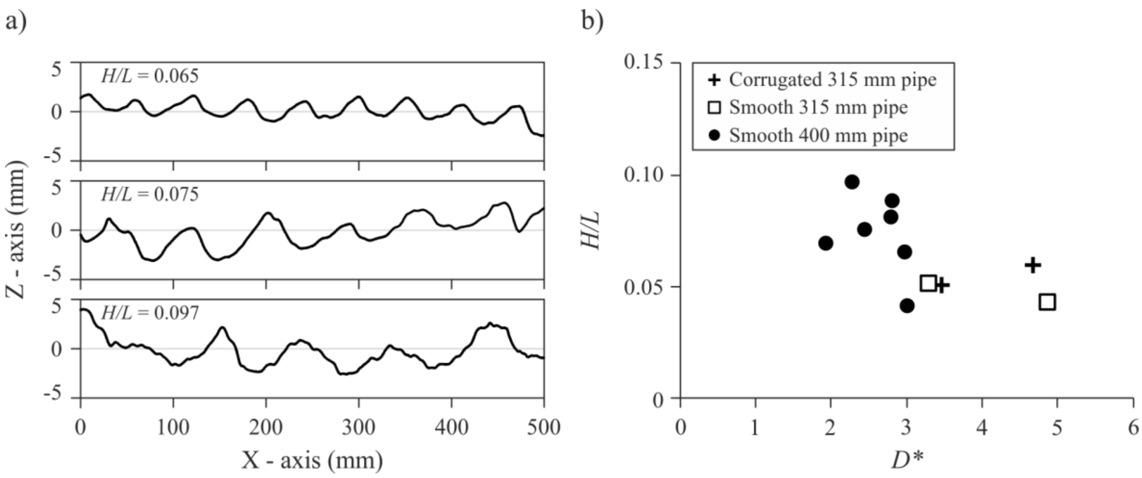

Figure 6. Longitudinal profiles after tests with H/L = 0.065, H/L = 0.075 and H/L = 0.097 (a) and bed form steepness as a function of the dimensionless particle diameter compared (b).

3.3.2. Flow resistance

Bed load transport prediction models are based on the relationship with the dimensionless bed shear stress $\theta_b = \tau_b/(g(\rho_s - \rho)d_{50})$. However, the development of bed forms in the sediment deposits produces variations in the bed shear stress that can spoil the sediment transport estimation. Therefore, the relationship between the dimensionless bed and skin friction shear stress, θ_b and θ_b' respectively, should be considered under the presence of bed formations. For instance, Ota and Nalluri (2003) presented the following relationship between θ_b and θ_b' based on experiments performed in a flume test facility with 225 and 305 mm pipes with uniform sand grain sizes ranging from 0.78 to 2.83 mm.

$$\theta_b = 18{\theta_b'}^{1.87} \qquad (6)$$

In this equation, the dimensionless bed shear stress increased due to the presence of dunes from a dimensionless shear value of 0.036. Engelund and Hansen (1967) also proposed a relationship between these two parameters based on sediment transport measurements in sand-bed streams. In the proposed equation the dimensionless bed shear stress differs from dimensionless skin friction shear stress, from 0.062 to 2.438.

$$\theta_b = \sqrt{\frac{\theta'_b - 0.06}{0.4}} \qquad (7)$$

Figure 7 shows the comparison between the dimensionless bed and skin friction shear stress in the present study. Both parameters are roughly equal for the bed flat conditions. Conversely, the local bed shear stress provided by the ADV presents slightly higher results when the bed forms occurred. Nevertheless, the deviation between θ_b and θ_b' was smaller than the relationship provided by the previous equations. This disagreement may have occurred because the sediments used in the experiments performed to obtain the equations 6) and 7) were non-cohesive sands in comparison with the fine cohesive sediments used in the present study. A similar tendency was shown in Banasiak and Verhoeven (2008), where results for non-cohesive sediments agreed with these experimental formulations, whereas partly cohesive surrogate mixtures presented lower differences between θ_b and θ'_b.

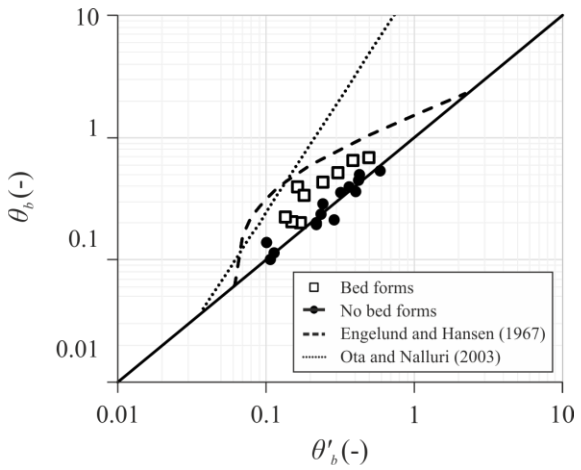

Figure 7. Measured dimensionless bed and skin friction shear stress and calculated values from the approaches of Engelund and Hansen (1967) and Ota and Nalluri (2003).

3.3.3. Bed load sediment transport rates

The bed-load transport q_b (g/m/s) was obtained from the difference between the final and the initial mass of bed deposits in the control section per width unit for each erosion step. This transport mode indicates the mobilization of bed deposits and is usually predicted by using the skin friction shear stress criteria τ'_b (Meyer-Peter and Müller, 1948). Figure 8 (a, b and c) shows the relationship between q_b and τ'_b parameters, highlighting the experiments with three erosion steps. A clear dependency is observed between the mobilised sediments and the preceding deposition phase. As an example, transport tests performed with 3-day deposited sediments under low shear stress conditions showed bed-load transport rates higher than those obtained after larger deposition periods. Under these non-consolidated conditions, the maximum sediment transport was exceeded in the second erosion step. After that, the available sediment in the pipe invert was insufficient to study the erosion processes in the third step. This lack of bed deposits in the control section was caused by a progressive erosion in the bed structure without a sediment supply from the inlet of the pipes, which was limited by the length of the flume test facility. Furthermore, q_b and τ'_b values were compared with a polynomial curve generated from the results of a study by Banasiak and Verhoeven (2008) for sands. This comparison illustrates that non-consolidated organic bed deposits present similar behaviour to sands. Therefore, sewer sediments showed non-cohesive behaviour under small preceding deposition times. However, as the consolidation time increased, the bed-load transport approach for sands overestimated the relationship between the initial sewer sediment mobilisation and the critical shear stress.

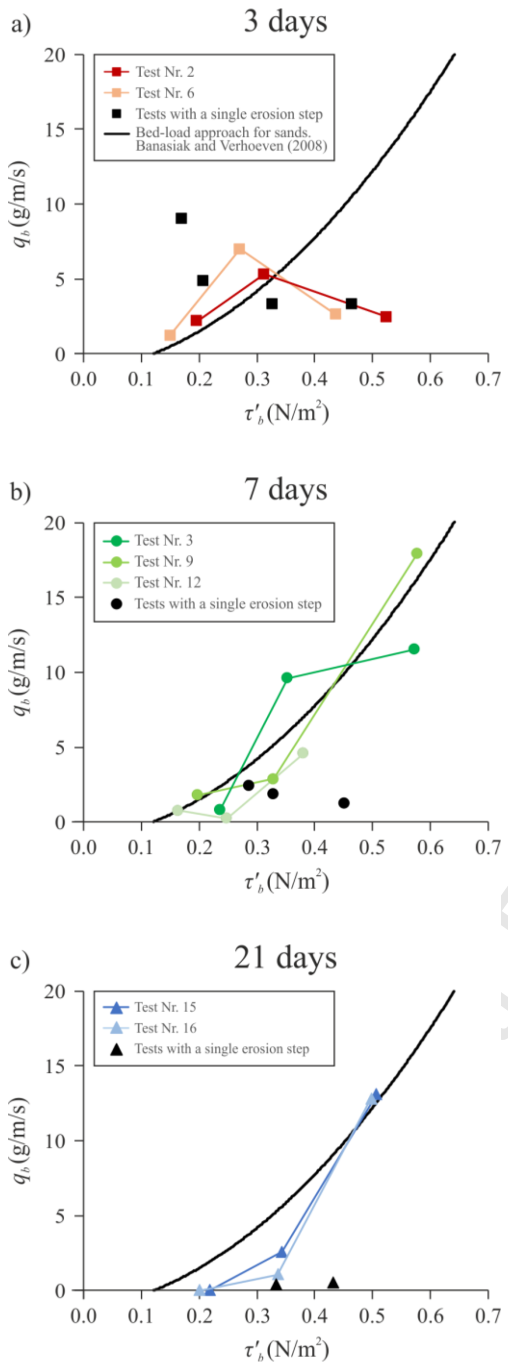

Figure 8. Bed-load transport and skin friction shear stress values for the erosion tests after preceding deposition times of 3 (a), 7 (b) and 21 (c) days, and comparison with the bed-load approach for sands from Banasiak and Verhoeven (2008) (black line). Erosion test identification numbers follow the numbering in Table S2 of the Supplementary Information to this article.

The critical bed shear stress can be roughly estimated at between ~0.15 and ~0.20 N/m^2 in the erosion tests with low deposition periods, which matches the highest percentages of volatile solids in bed deposits. This parameter varied considerably between ~0.16 and ~0.24 N/m^2 when the preceding deposition time was 7 days. Finally, the erosion tests with 21 days preceding accumulation phase presented the lowest amounts of organic contents and the critical bed shear stress was higher than ~0.30 N/m^2. Therefore, longer periods of deposition favour bed deposit cohesion, resulting in greater bed resistance. Likewise, sediment cohesion is related to the transformation of the organic matter due to the dependency between the accumulation time and the evolution of the organic content, as seen in the accumulation tests.

In order to compare these erosion results with most previous bed-load transport studies, Figure 9 sets out the relationship between the dimensionless skin friction shear stress θ'_b and the dimensionless bed-load transport $\phi_b = q_b/\left(\rho_s\left(gd_{50}^3(\rho_s-\rho)/\rho\right)^{0.5}\right)$. Erosion tests were classified based on the disturbance depth. The disturbance depth δ (mm), which is defined as the difference between the final and the initial sediment heights, represents another meaningful parameter to assess the erodibility of bed deposits (Banasiak and Verhoeven, 2008). A disturbance depth limit of 5 mm was fixed to classify the erosion tests. Below this limit, erosion tests showed ϕ_b values without a clear pattern. This spread of results corresponded mainly to experiments with small initial sediment heights. Because of the lack of sediment at the beginning of the erosion test, a swift erosion of the bed deposits could be expected and, therefore, the bed-load transport rate would be underestimated. Under such conditions, a better approach would be provided by erosion rate formulas. No other correlation was identified between these results and the remaining sediment parameters mentioned. On the other hand, tests with disturbance depths higher than 5 mm followed a potential approach, similar to most previous studies. Above this limit, it was assumed that the bed-load transport conditions had developed over the course of the erosion test.

The bed-load transport results were also compared to those obtained from other existing bed-load transport models, hereafter $\phi_b - \theta'_b$ models. In order to simplify this comparison, two ϕ_b – θ'_b models were presented, which resulted from experiments with non-cohesive and organic mixtures, respectively. Ota and Nalluri (2003) presented an equation based on uniform sand studies, in which the dimensionless bed transport parameter was obtained by the difference between the dimensionless skin friction and critical bed shear stress:

$$\phi_b = 16.5(\theta'_b - 0.036)^{1.67} \tag{8}$$

The value of the critical dimensionless bed shear stress was fixed at 0.036, lower than 0.047 proposed by Meyer-Peter and Müller (1948). According to the present results, this model overestimates the dimensionless bed transport parameter. Banasiak and Verhoeven (2008) showed that bed transport was predicted accurately by this model for non-cohesive sediments. However, sediment transport was also overestimated in the experiments with cohesive mixtures. Conversely, Arthur et al. (1996) proposed a model to predict the transport of near-bed fluid sediments based on measurements in real sewers.

$$\phi_b = 2.2775 \times 10^{-3} \theta'^{2.2}_b D_*^{0.38} Z^{-1.11} (B/hw)^{0.78} \tag{9}$$

where $Z = d_{50}/hw$ is the relative grain size and h_w the flow depth. This $\phi_b - \theta'_b$ model derives from the modification of the inorganic near bed transport rate model proposed previously by Perrusquia and Nalluri (1995). The model yields better performance with the results that showed a significant disturbance depth in the present study. The main reason for this agreement is that the above equation was obtained from measurements with organic material.

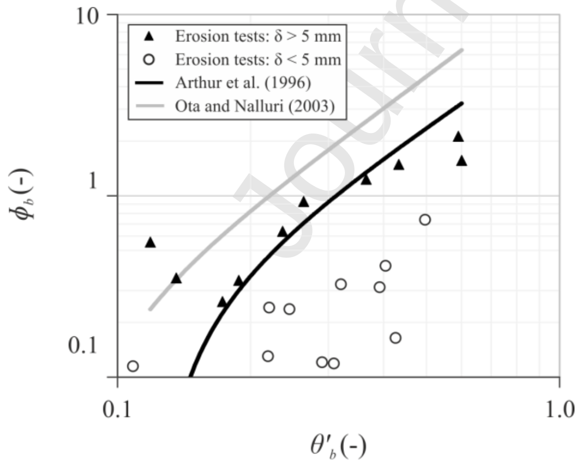

Figure 9. Measured dimensionless bed transport and skin friction shear stress, and values calculated from the approaches of Arthur et al. (1996) and Ota and Nalluri (2003).

4. DISCUSSION

Previous erosion and transport studies were mostly performed in laboratory flumes with tap water and granular, non-cohesive materials. Therefore, equations for the study of sewer sediment transport were generally drawn from river research (Bertrand-Krajewski, 2006). However, field studies typically defined sewer sediments as cohesive mixtures with a significant percentage of organic matter. Recent laboratory work has been carried out with surrogate organic materials or cohesive mixtures in order to bring sediment transport models nearer to real sewer conditions. Nevertheless, these studies have also presented some limitations since they only consider the erosion and transport phases, ignoring previous in-sewer deposition processes. The current study presents an experimental campaign performed in a flume test facility in order to study the deposition and erosion processes in sewer pipes. The facility has the advantage that wastewater can be supplied to the experimental facility. Under these conditions, deposited sediments presented organic contents higher than 10%, similar to those obtained in field research.

Short and long accumulation periods were planned in the experimental campaign in order to study the deposition mode depending on the pipe diameter and the wastewater supply conditions, and the influence of sediment consolidation in the subsequent enforced mobilization of bed sediments. On the other hand, erosion tests were designed to analyse the flow resistance regarding formations in the surface of deposited sediments. Furthermore, some erosion tests were performed under increasing flow velocity steps in order to determine the sediment motion threshold. For all experiments, inlet conditions were monitored and the bed structure and its physicochemical properties were measured with a high degree of accuracy. New insights have been developed here to analyse the physicochemical properties of deposited mixtures and to measure the transported sediments.

Physicochemical analyses of the sewer sediments were performed during the accumulation tests. Two types of sediments were observed in the pipes, following the classification of Crabtree (1989). Bed deposits were classified as non-uniform mixtures of Type A/C. These mixtures were mainly formed by fine-grained and granular materials. The percentage of fine particles (< 63 µm) ranged from 25% to 30%, and thus bed deposits could be assumed to be cohesive mixtures (Torfs et al., 1994). Fine grain sizes are relevant since they lead to more cohesive structures of bed deposits, and their resistance has an influence on erosion (Banasiak and Verhoeven, 2008). On the other hand, biofilms of Type D developed on the pipe walls, from the wastewater surface to the bed deposits. The organic fraction of these sediments was higher than bed deposits, and their composition showed silt particles and greases. Because of both deposition classes, the pipe roughness was modified and the sediment transport capacity of the sewer pipes decreased.

Average values from the physicochemical analyses were broadly in line with reference studies, except for the COD values, which were lower, especially for biofilms. Negligible deviations were found between the sediments sampled in the different circular pipe configurations. Also, a significant variability in bed deposit and wall biofilm properties was obtained in relation to the deposition time. This variability was caused by biological processes within the sediments and their interaction with the wastewater flow (Crabtree, 1989). The main effect of the 'aging' of this sediment was the increase in density and solid content and, conversely, the reduction in organic matter and mean grain size of the bed deposits. Results from the analysis of volatile solids, COD and OUR attained their maximum values during the first days of deposition. The same trends were reported by Ristenpart (1995), who analysed bed deposit samples at different deposition stages from an intercept sewer.

COD type I values showed the total pollution of the sample, in that the blending process separates the polluted fraction from the solid particles, following McGregor et al. (1993). Also, the COD type II and III accounted for the readily erodible fraction of pollutants that could be released from the sample. Ashley et al. (2004) showed that the fractions between the COD obtained from the readily erodible and blending preparation processes were 25% and 57% for type A and C sediments, respectively. Current results showed that 74% of the pollutants attached to the sediment could be discharged into the wastewater during the first accumulation days, this produced by a shear stress increase. After several weeks, this percentage was slightly reduced to 56%, close to levels reported by Ashley et al. (2004). In the case of wall biofilms, this fraction was roughly constant, and higher than 75%. On the other hand, the biological activity of the sediment sample was evaluated with the OUR. High OUR values pointed to a high percentage of organic matter and also a rapid biodegradation of the sediment sample, which could be related to the sediment bed resistance, according to previous studies (c.f. Vollertsen and Hvitved-Jacobsen 2000).

In addition to the methodologies used to characterize the sediment properties, an innovative photogrammetric technique was also developed for measuring the deposited sediments in pipes. The SfM was used to perform a 3D reconstruction of the sediment surface, detailing the bed structures. Within the area of sediment transport in sewers, no similar studies have been found that apply this photogrammetric methodology. Although the application of SfM in the laboratory flume was simple, its implementation in field studies might be less effective due to the draining phase of the pipes. The most frequently used techniques in field campaigns were based on multiple point measurements or transversal profilers, such as laser or sonar technologies (Bertrand-Krajewski and Gibello, 2008; Lepot et al., 2017). Furthermore, computational vision techniques were also developed to record bed load transport through longitudinal sections (Grasso et al., 2017). However, previous techniques missed part of the bed surface information, and presented high-level data processing.

Periodical SfM measurements made it possible to monitor the progressive deposition of sediments during the accumulation tests. The accumulation was influenced by the flow velocity and the inlet suspended solid conditions, which depended on the wastewater supply conditions. The raw wastewater system introduced higher suspended solid concentrations than the pressurized system. Therefore, the highest bed depositions were produced by the highest concentrations, together with the lowest velocities. The resulting daily rates during the first deposition week ranged between 1.3 and 6.2 mm/d (0.078 and 0.997 kg/m/d) for the 315 mm smooth and corrugated pipes, and between 0.8 and 4.1 mm/d (0.070 and 0.508 kg/m/d) for the 400 mm smooth pipe. Under similar test conditions, Lange and Wichern (2013) showed an average daily accumulation of 2.85 mm/d. Earlier studies, such as Verbanck (1992), reported daily deposition rates in combined sewers of between 0.154 and 0.176 kg/m/d.

The accuracy of the SfM methodology also allowed for the assessment of bed forms characteristics. These formations were developed in some of the erosion tests with Froude numbers between 0.3 and 0.5. Most of the observed bed forms corresponded to ripples, as they satisfied the shear velocity Reynolds number criteria proposed by Garcia (2008). In the tests with Froude numbers close to 0.5, transition towards dunes were identified.

Ripple forms depend mainly on the bed deposit characteristics. Because of this, it was found that the dimensionless particle diameter increased as the bed form steepness decreased. Past studies, such as Raudkivi (1997), showed the same trend. Nevertheless, the measured bed forms were smaller than those observed in studies with only granular materials (Banasiak and Verhoeven, 2008), this due mainly to the cohesion of the sewer sediment. Therefore, prediction formulas for ripple dimensions, which typically depend on the mean grain size (c.f. Julien and Klaassen, 1995; Baas, 1999), provided wide differences.

Total bed shear stress, which was obtained from the turbulent profile recorded with the ADV, was influenced by the bed forms regarding flat bed conditions. Results showed small differences between the skin friction and the bed shear stress when ripples were formed, which implied a higher bed resistance. The equations proposed by Engelund and Hansen (1967) and Ota and Nalluri (2003) to estimate this deviation between the shear stresses were formulated from tests performed with non-cohesive granular sediments. Both equations produced greater differences in comparison to the measurements themselves. Similar behaviour was reported by Banasiak and Verhoeven (2008), where it was suggested that the cohesive mixtures significatively reduce this deviation.

Differences between bed structures at the beginning and end of the erosion steps were used to measure sediment transport. The calculation of the eroded mass in the control section was improved due to the SfM methodology. The erosion mode was identified as bed-load transport because no significant shifts were recorded in the wastewater loads at the flume outlet. This transport mode was affected by the preceding deposition time of the sewer sediments. Freshly deposited sediments behaved like non-cohesive granular material, despite the high percentage of fine particles. As the accumulation time increased, bed deposits tended to consolidate (Banasiak et al., 2005), increasing their cohesion and so their erosion threshold. This behaviour derived in lower bed-load transport rates for the same grain shear stress conditions. Also, critical shear stress could be assumed to be higher when the deposition time increased, which was also in line with the increase in particle density and the reduction of organic matter. Therefore, the erodibility of the bed deposits was directly affected by the variation of the sediment properties due to the consolidation period. During this period, the formation of EPS and the microbial community activity can also play an important role in sediment anti-scouribility (Meng *et al.* 2019).

The relationship between the dimensionless bed-load transport rate and skin friction shear stress measurements seemed to be randomly spread. Thus, a disturbance-depth-based criterion was selected to discern a relationship between the results and the common sediment transport capacity formulas. The disturbance depth δ has frequently been used to assess sediment erodibility and particle re-entraining during the transport processes (Ashley et al., 2004; Banasiak and Verhoeven, 2008). In the present study, a disturbance depth higher than 5 mm was considered to ensure continuous bed-load transport conditions during a single erosion step. Conversely, δ < 5 mm were mainly obtained from tests with residual amounts of bed deposits at the beginning of the step, which behaved like difficult-to-wash crusts. These tests were affected by the progressive erosion of bed deposits upstream of the control section, which was limited by the flume length. Thus, the time to reach the bed-load equilibrium was less than the step duration and, consequently, the uncertainty of the sediment transport measurement increased. In these tests, sediment mobility could be influenced more by erosion-based processes of cohesive sediments, whilst transport capacity formulas seemed to provide unreliable predictions.

After establishing the disturbance depth criteria, $\phi_b - \theta'_b$ measurements from the erosion tests with a δ > 5 mm broadly agreed with the formula proposed by Arthur et al. (1996). This approach was based on organic bed-load transport measurements in a real sewer and showed a better performance in comparison with other models, such as Ota and Nalluri (2003), which was formulated after performing erosion tests with non-cohesive and uniform materials. On the other hand, dimensionless bed-load transport rates were overestimated by previous $\phi_b - \theta'_b$ models in the erosion tests, in which the δ < 5 mm condition was satisfied.

5. CONCLUSIONS

A series of sediment accumulation and transport tests were performed in different circular pipes, placed in a flume test facility. New insights were developed towards sewer sediment transport analysis. The photogrammetric technique SfM allowed for the highly accurate measurement of the volume and the bed forms of the deposited sediments. Results from this technique improved the information about the bed structure in comparison to punctual or transversal profile measurements. Another methodology developed in this study was the physicochemical characterization of sediment samples in both accumulation and erosion tests. These analyses made it possible to study the evolution of the sediment properties and their influence in the bed resistance. Organic matter indicators, such as COD or OUR, pointed to the biological processes of the sediment sample.

Accumulation tests showed that the increase of the deposition in the pipes followed a linear trend within the first week. Later, the sediment height tended towards a constant value. However, this value decreased in some cases due to compacting processes in the bed deposits. Furthermore, the deposition time had an influence in the variation of the physicochemical properties of bed deposits and, to a lesser extent, in wall biofilms. As the deposition advanced, biological transformations reduced the organic fraction of the sediment samples, pointing to continuous biodegradation.

Erosion tests were performed to quantify the bed resistance and the sediment transport in circular pipes. Bed forms were developed in some of these tests with Froude numbers between 0.3 and 0.5. The bed shear stress produced by the bed forms was slightly higher in comparison with flat bed conditions. This difference strongly affected bed resistance. Furthermore, a clear relationship was observed between the bed-load transport rates, the deposition time, and the biological transformations of the sewer sediments. Bed deposits were easily eroded after short accumulation periods, showing a similar behaviour to non-cohesive mixtures. Conversely, higher critical bed shear stress values were obtained for consolidated sediments, pointing to greater cohesion. Therefore, long dry weather periods in combined sewers with sediment deposition would increase bed deposit resistance, thus hindering sediment erosion.

Finally, bed-load transport rates were generally overestimated with transport capacity formulas. Only a potential curve trend was found between the dimensionless skin friction shear stress and bed-load transport results when the eroded depth was significant ($\delta > 5$ mm). Under these conditions, the formula presented by Arthur et al. (1996) provided suitable predictions, since it derived from studies with cohesive organic sediments. However, the lack of formulas to predict the transport of organic and cohesive sediments in sewer pipes is still missing. Future work should focus on improvements in the measurement of the sediment threshold motion and the erosion time, in order to avoid the complete bed deposit erosion being below the testing time.

6. ACKOWLEDGEMENTS

This research was financed by the projects ‘SEDUNIT’ Ref. CGL2015-69094-R and ‘OVALPIPE II’ Ref. RTC-2016-4987-5 (MINECO/FEDER, EU). The authors would like to thank the companies

EDAR Bens SA, EMALCSA and ABN Pipe Systems S.L.U. for their assistance with the experimental work.

7. REFERENCES

Ackers, J.C., Butler D. & May R.W.P. (1996). *Design of sewers to control sediment problems*. CIRIA Report R141, London, U.K.

AENOR (2014). *UNE-EN 1097-6:2014. Tests for mechanical and physical properties of aggregates. Part6: Determination of particle density and water absorption*. Asociación Española de Normalización y Certificación, Madrid, Spain.

Ahyerre, M., Chebbo, G. & Saad, M. (2001). Nature and dynamics of water sediment interface in combined sewers. *J. Environ. Eng*. **127**(3), 233-239. https://doi.org/10.1061/(ASCE)0733-9372(2001)127:3(233)

APHA, AWWA & WEF (1998). *Standard Methods for the Examination of Water and Wastewater*. 20th edn, American Public Health Association/American Water Works Association/Water Environment Federation, Washington DC, USA.

Arthur, S., Ashley, R.M. & Nalluri, C. (1996). Near bed solids transport in sewers. *Wat. Sci. Technol*. **33**(9), 69-76. https://doi.org/10.1016/0273-1223(96)00371-X

Ashley, R., Bertrand-Krajewski, J.L., Hvitved-Jacobsen, T. & Verbanck, M. (2004). *Solids in sewers. Scientific & Technical Report No. 14*. IWA Publishing, London, UK.

Ashley, R.M. & Crabtree, R.W. (1992). Sediment origins, deposition and build-up in combined sewer systems. *Wat. Sci. Technol*. **25**(8), 1-12. https://doi.org/10.2166/wst.1992.0173

Baas, J.H. (1999). An empirical model for the development and equilibrium morphology of current ripples in fine sand. *Sedimentology*. **46**(1), 123-138. https://doi.org/10.1046/j.1365-3091.1999.00206.x

Banasiak, R. & Verhoeven, R. (2008). Transport of sand and partly cohesive sediments in a circular pipe run partially full. *J. Hydraul. Eng.* **134**(2), 216-224. https://doi.org/10.1061/(ASCE)0733-9429(2008)134:2(216)

Banasiak, R., Verhoeven, R., De Sutter, R. & Tait, S. (2005). The erosion behaviour of biologically active sewer sediment deposits: observations from a laboratory study. *Water Res*. **39**(20), 5221-5231. https://doi.org/10.1016/j.watres.2005.10.011

Bertrand-Krajewski, J.L. (2006). *Modelling of Sewer Solids Production and Transport. Cours de DEA "Hydrologie Urbaine"*, Transport. INSA de Lyon, Lyon, France.

Bertrand-Krajewski, J.L. & Gibello, C. (2008). A new technique to measure cross-section and longitudinal sediment profiles in sewers. In *11th International Conference on Urban Drainage*, Edinburgh, Scotland, UK.

Campisano, A., Creaco, E. & Modica, C. (2008). Laboratory investigation on the effects of flushes on cohesive sediment beds. *Urban Water J.*, **5**(1), 3-14. https://doi.org/10.1080/15730620701726259

Chebbo, G. & Bachoc, A. (1992). Characterization of suspended solids in urban wet weather discharges. *Wat. Sci. Technol*. **25**(8), 171-179. https://doi.org/10.2166/wst.1992.0191

Crabtree, R. W. (1989). Sediments in sewers. *Water Environ. J.* **3**(6), 569-578. https://doi.org/10.1111/j.1747-6593.1989.tb01437.x

De Sutter, R. (2000). *Erosion and transport of cohesive sediment mixtures in unsteady flow (Doctoral dissertation*, PhD thesis. Gent Universiteit, Gent, Belgium.

De Sutter, R., Rushforth, P., Tait, S., Huygens, M., Verhoeven, R. & Saul, A. (2003). Validation of existing bed load transport formulas using in-sewer sediment. *J. Hydraul. Eng.* **129**(4), 325-333. https://doi.org/10.1061/(ASCE)0733-9429(2003)129:4(325)

Del Río, H., Suárez, J., Puertas, J. & Ures, P. (2013). PPCPs wet weather mobilization in a combined sewer in NW Spain. *Sci. Total Environ.* **449**, 189-198. https://doi.org/10.1016/j.scitotenv.2013.01.049

Einstein, H.A. (1942). Formulas for bed-load transportation. *Trans. ASCE*, 107, 561–597, USA.

Engelund, F. & Hansen, E. (1967). *A monograph on sediment transport in alluvial streams*. TekniskForlag, Copenhagen, Denmark.

Garcia, M. (2008). *Sedimentation engineering: processes, measurements, modeling, and practice*. American Society of Civil Engineers, Virginia, U.S.A.

Goring, D.G. & Nikora, V.I. (2002). Despiking acoustic Doppler velocimeter data. *J. Hydraul. Eng*. **128**(1), 117-126. https://doi.org/10.1061/(ASCE)0733-9429(2002)128:1(117)

Grasso, M., Giudice, O., Campisano, A., Shahsavari, G., Battiato, S. & Modica, C. (2017). Testing Computer Vision techniques for bedload sediment transport evaluation in sewers. In *14th IWA/IAHR International Conference on Urban Drainage*, Prague, Czech Republic.

Gromaire, M.C., Garnaud, S., Saad, M. & Chebbo, G. (2001). Contribution of different sources to the pollution of wet weather flows in combined sewers. *Water Res*. **35**(2), 521-533. https://doi.org/10.1016/S0043-1354(00)00261-X

Houhou, J., Lartiges, B.S., Montarges-Pelletier, E., Sieliechi, J., Ghanbaja, J. & Kohler, A. (2009). Sources, nature, and fate of heavy metal-bearing particles in the sewer system. *Sci Total Environ.* **407**(23), 6052-6062. https://doi.org/10.1016/j.scitotenv.2009.08.019

ISO (2009). *ISO 13320:2009. Particle size analysis. Laser diffraction methods.* International Organization for Standardization, Geneva, Switzerland.

Julien, P.Y. & Klaassen, G.J. (1995). Sand-dune geometry of large rivers during floods. *J. Hydraul. Eng*. **121**(9), 657-663. https://doi.org/10.1061/(ASCE)0733-9429(1995)121:9(657)

Khastar-Boroujeni, M., Esmaili, K., Samadi-Boroujeni, H. & Ziaei, A. (2017). Wastewater Effect on the Deposition of Cohesive Sediment. *J. Environ. Eng*. **144**(1), 04017083. https://doi.org/10.1061/(ASCE)EE.1943-7870.0001270

Lange, R.L. & Wichern, M. (2013). Sedimentation dynamics in combined sewer systems. *Wat. Sci. Technol*. **68**(4), 756-762. https://doi.org/10.2166/wst.2013.278

Lepot, M., Pouzol, T., Aldea-Borruel, X., Suner, D. & Bertrand-Krajewski, J.L. (2017). Measurement of sewer sediments with acoustic technology: from laboratory to field experiments. *Urban Water J*. **14**(4), 369-377. https://doi.org/10.1080/1573062X.2016.1148181

Maa, J.P.Y., Kwon, J.I., Hwang, K.N. & Ha, H.K. (2008). Critical bed-shear stress for cohesive sediment deposition under steady flows. *J. Hydraul. Eng*. **134**(12), 1767-1771. https://doi.org/10.1061/(ASCE)0733-9429(2008)134:12(1767)

May, R.W. (1993). *Sediment transport in pipes, sewers and deposited beds*. Rep. No. SR 320. HR Wallingford Ltd., Wallingford, U.K.

McGregor, I., Ashley, R. M. & Oduyemi, K. K. (1993). Pollutant release from sediments in sewer systems and their potential for release into receiving waters. *Wat. Sci. Technol*. **28**(8/9), 161-169. https://doi.org/10.2166/wst.1993.0614

Meng, D., Wu, J., Chen, K., Li, H., Jin, W., Shu, S. & Zhang, J. (2019). Effects of extracellular polymeric substances and microbial community on the anti-scouribility of sewer sediment. *Sci. Total Environ.* **687**, 494-504. https://doi.org/10.1016/j.scitotenv.2019.05.387

Meyer-Peter, E. & Müller, R. (1948). *Formulas for bed-load transport*. In IAHSR 2nd meeting, appendix 2. IAHR, Stockholm, Sweden.

Miller, J.D. & Hutchins, M. (2017). The impacts of urbanisation and climate change on urban flooding and urban water quality: A review of the evidence concerning the United Kingdom. *J. Hydrol. Reg. Stud.* **12**, 345-362. https://doi.org/10.1016/j.ejrh.2017.06.006

Munro, K., Martins, C.P., Loewenthal, M., Comber, S., Cowan, D.A., Pereira, L. & Barron, L.P. (2019). Evaluation of combined sewer overflow impacts on short-term pharmaceutical and illicit drug occurrence in a heavily urbanised tidal river catchment (London, UK). *Sci. Total Environ.* **657**, 1099-1111. https://doi.org/10.1016/j.scitotenv.2018.12.108

Nalluri, C., Ghani, A.A. & El-Zaemey, A.S. (1994). Sediment transport over deposited beds in sewers. *Wat. Sci. Technol*. **29**(1-2), 125-133. https://doi.org/10.2166/wst.1994.0658

Naves, J., Anta, J., Puertas, J., Regueiro-Picallo, M. & Suárez, J. (2019a). Using a 2D shallow water model to assess Large-Scale Particle Image Velocimetry (LSPIV) and Structure from Motion (SfM) techniques in a street-scale urban drainage physical model. *J. Hydrol*. **575**, 54-65. https://doi.org/10.1016/j.jhydrol.2019.05.003

Naves, J., Anta, J., Regueiro-Picallo, M., Suárez, J. & Puertas, J. (2019b). WASHTREET. Application of Structure from Motion (SfM) photogrammetric technique to determine surface elevations in an urban drainage physical model. [Data set]. Zenodo. http://doi.org/10.5281/zenodo.3241337

Oms, C., Gromaire, M.C., Saad, M., Milisic, V. & Chebbo, G. (2008). Bed shear stress evaluation in combined sewers. *Urban Water J*. **5**(3), 219-229. https://doi.org/10.1080/15730620801924010

Ota, J.J. & Nalluri, C. (2003). Urban storm sewer design: Approach in consideration of sediments. *J. Hydraul. Eng*. **129**(4), 291-297. https://doi.org/10.1061/(ASCE)0733-9429(2003)129:4(291)

Perrusquia, G.S. (1992). An experimental study on the transport of sediment in sewer pipes with a permanent deposit. *Wat. Sci. Technol.* **25**(8), 115-122. https://doi.org/10.2166/wst.1992.0185

Perrusquia, G. & Nalluri, C. (1995). Modelling of bed-load transport in pipe channels. In *8th International Conference on Transport and Sedimentation of Solid Particles*, Prague, Czech Republic.

Rammal, M., Chebbo, G., Vazquez, J. & Joannis, C. (2017). Do storm events samples bias the comparison between sewers deposits contribution? *Wat. Sci. Technol.* **75**(2), 271-280. https://doi.org/10.2166/wst.2016.514

Raudkivi, A.J. (1997). Ripples on stream bed. *J. Hydraul. Eng*. **123**(1), 58-64. https://doi.org/10.1061/(ASCE)0733-9429(1997)123:1(58)

Regueiro-Picallo, M., Anta, J., Suárez, J., Puertas, J., Jácome, A. & Naves, J. (2018). Characterisation of sediments during transport of solids in circular sewer pipes. *Wat. Sci. Technol.* **2017**(1), 8-15. https://doi.org/10.2166/wst.2018.055

Regueiro-Picallo M., Naves, J., Anta, J., Suárez, J. & Puertas, J. (2017). Monitoring accumulation sediment characteristics in full scale sewer physical model with urban wastewater. *Wat. Sci. Technol.* **76**(1), 115-123. https://doi.org/10.2166/wst.2017.118

Ristenpart, E. (1995). Sediment properties and their changes in a sewer. *Wat. Sci. Technol*. **31**(7), 77-83. https://doi.org/10.1016/0273-1223(95)00325-H

Rocher, V., Azimi, S., Moilleron, R. & Chebbo, G. (2004). Hydrocarbons and heavy metals in the different sewer deposits in the 'Le Marais' catchment (Paris, France): stocks, distributions and origins. *Sci. Total Environ.* **323**(1-3), 107-122. https://doi.org/10.1016/j.scitotenv.2003.10.010

Rushforth, P.J., Tait, S.J. & Saul, A.J. (2003). Modeling the erosion of mixtures of organic and granular in-sewer sediments. *J. Hydraul. Eng.* **129**(4), 308-315. https://doi.org/10.1061/40583(275)49

Sadaka, S.S., Richard, T.L., Loecke, T.D. & Liebman, M. (2006). Determination of compost respiration rates using pressure sensors. *Compost Science & Utilization*. **14**(2), 124-131. https://doi.org/10.1080/1065657X.2006.10702273

Sakrabani, R., Ashley, R.M. & Vollertsen, J. (2005). The influence of biodegradability of sewer solids for the management of CSOs. *Wat. Sci. Technol*. **51**(2), 89-97. https://doi.org/10.2166/wst.2005.0036

Sakrabani, R., Vollertsen, J., Ashley, R.M. & Hvitved-Jacobsen, T. (2009). Biodegradability of organic matter associated with sewer sediments during first flush. *Sci. Total Environ*. **407**(8), 2989-2995. https://doi.org/10.1016/j.scitotenv.2009.01.008

Schellart, A., Veldkamp, R., Klootwijk, M., Clemens, F.H.L.R., Tait, S., Ashley, R. & Howes, C. (2005). Detailed observation and measurement of sewer sediment erosion under aerobic and anaerobic conditions. *Wat. Sci. Technol*. **52**(3), 137-146. https://doi.org/10.2166/wst.2005.0070

Schertzinger, G., Itzel, F., Kerstein, J., Tuerk, J., Schmidt, T.C. & Sures, B. (2019). Accumulation pattern and possible adverse effects of organic pollutants in sediments downstream of combined sewer overflows. *Sci. Total Environ.* **675**, 295-304. https://doi.org/10.1016/j.scitotenv.2019.04.094

Seco, I., Valentín, M.G., Schellart, A. & Tait, S. (2014). Erosion resistance and behaviour of highly organic in-sewer sediment. *Wat. Sci. Technol*. **69**(3), 672-679. https://doi.org/10.2166/wst.2013.761

Skipworth, P.J., Tait, S.J. & Saul, A.J. (1999). Erosion of sediment beds in sewers: Model development. *J. Environ. Eng*. **125**(6), 566-573. https://doi.org/10.1061/(ASCE)0733-9372(1999)125:6(566)

Suarez, J. & Puertas, J. (2005). Determination of COD, BOD, and suspended solids loads during combined sewer overflow (CSO) events in some combined catchments in Spain. *Ecological Engineering*. **24**(3), 199-217. https://doi.org/10.1016/j.ecoleng.2004.11.005

Tait, S.J., Chebbo, G., Skipworth, P.J., Ahyerre, M. & Saul, A.J. (2003). Modeling in-sewer deposit erosion to predict sewer flow quality. *J. Hydraul. Eng.* **129**(4), 316-324. https://doi.org/10.1061/(ASCE)0733-9429(2003)129:4(316)

Tait, S.J., Rushforth, P.J. & Saul, A. J. (1998). A laboratory study of the erosion and transport of cohesive-like sediment mixtures in sewers. *Wat. Sci. Technol*. **37**(1), 163-170. https://doi.org/10.1016/S0273-1223(97)00766-X

Torfs, H., Huygens, M. & Tito, L. (1994). Influence of the cross-section on the erosion criteria for partly cohesive sediments. *Wat. Sci. Technol*. **29**(1-2), 103-111. https://doi.org/10.2166/wst.1994.0656

Van Rijn, L.C. (1984). Sediment transport, part III: bed forms and alluvial roughness. *J. Hydraul. Eng*. **110**(12), 1733-1754. https://doi.org/10.1061/(ASCE)0733-9429(1984)110:12(1733)

Verbanck, M. (1990). Sewer sediment and its relation with the quality characteristics of combined sewer flows. *Wat. Sci. Technol.* **22**(10-11), 247-257. https://doi.org/10.2166/wst.1990.0311

Verbanck, M. (1992). Field investigations on sediment occurrence and behaviour in Brussels combined sewers. *Wat. Sci. Technol*. **25**(8), 71-82. https://doi.org/10.2166/wst.1992.0181

Vollertsen, J. & Hvitved-Jacobsen, T. (2000). Resuspension and oxygen uptake of sediments in combined sewers. *Urban Water*. **2**(1), 21-27. https://doi.org/10.1016/S1462-0758(00)00036-4

Declaration of interests

☒ The authors declare that they have no known competing financial interests or personal relationships that could have appeared to influence the work reported in this paper.

☐The authors declare the following financial interests/personal relationships which may be considered as potential competing interests:

Graphical abstract

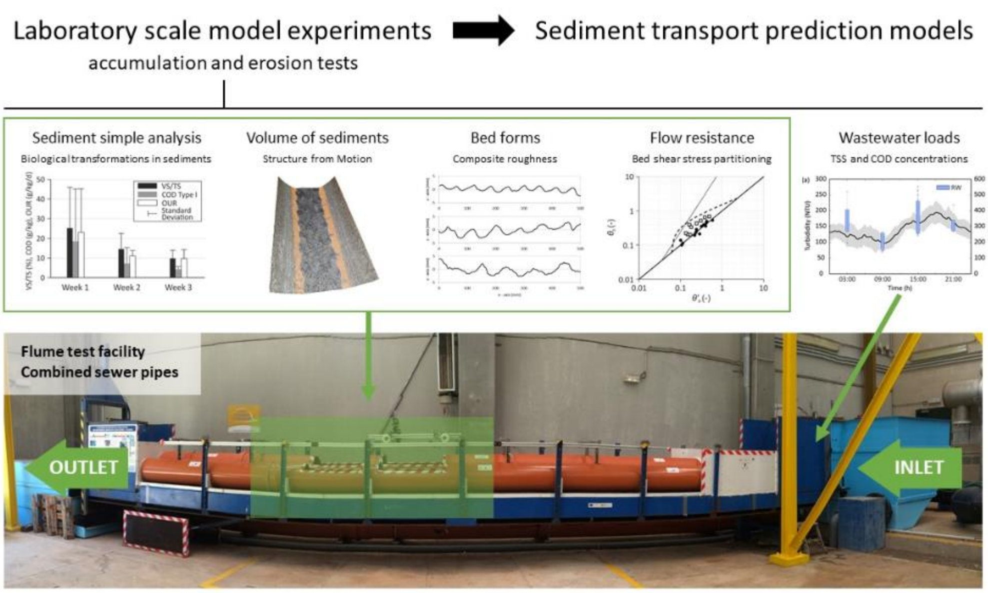

HIGHLIGHTS

- Accumulation and transport experiments were performed in combined sewer pipes
- Photogrammetric techniques improve the measurement of deposited sediments
- Bed resistance is influenced by the presence of organic and cohesive materials
- Deposition processes produce transformations in sewer sediment properties
- The influence of deposition times should be considered in sediment transport models